AIAA JOURNAL
Vol. 38, No. 1, January 2000

Rotor Wake Modeling for Flight Dynamic Simulation of Helicopters

Richard E. Brown*
University of Glasgow, Glasgow, Scotland G12 8QQ, United Kingdom

A computational helicopter rotor wake model, based on the numerical solution of the unsteady fluid-dynamic equations governing the generation and convection of vorticity through a domain enclosing the helicopter, has been developed. The model addresses several issues of specific interest in the context of helicopter flight dynamic modeling. The problem of excessive numerical dissipation of vortical structure, common to most grid-based computational techniques, is overcome using a vorticity conservation approach in conjunction with suitable vorticity-flux limiter functions. Use of a time-factorization-type algorithm allows the wake model to avoid the stiffness that is introduced in flight dynamic applications by the disparity between the rotor and fuselage timescales and to generate rapid solutions to the time-varying vortical structure of the helicopter wake. The model is demonstrated to yield valid solutions to the blade loading and wake structure for isolated and interacting rotors in both hover and forward flight.

Nomenclature

B = domain of inner aerodynamic problem
$\boldsymbol{b}$ = vector of airframe and rotor states
c = blade chord
k = reduced frequency of pitching oscillation
M = number of substeps
N = problem size
R = rotor radius
r = radial coordinate
S = source of vorticity
T = rotor period of revolution, period of pitching oscillation
t = time
U = freestream velocity, velocity at blade section
V = fluid domain
V' = computational domain
v = velocity of flow
Δt = computational timestep
ν = frequency of pitch oscillation
ω = flow vorticity

Introduction

THE earliest model for the dynamics of the induced flow near a helicopter rotor was developed by Carpenter and Fridovich,[1] who introduced a term representing the acceleration of a mass of air surrounding the rotor into their momentum-disk-type model to explain their observations of first-order dynamics of the induced velocity below a hovering rotor. Subsequently, Gaonkar and Peters[2] and Peters et al.[3] developed more general, first-order, disk-type dynamic theories for the induced flow, based more rigorously on considerations of the pressure distribution on the rotor disk. The Peters-type dynamic inflow theories have been developed[2] over the last two decades to an impressive level of sophistication, where the effects of individual blades[3] on the induced velocity distribution on the rotor disk can now be incorporated. Dynamic inflow models are now widely used, despite some shortcomings,[4] in the current generation of computational helicopter flight dynamics models.[5,6]

During the past few years a gathering body of evidence has suggested that the detailed geometry and strength of the wake shed by the various aerodynamic components of a helicopter has a significant impact on the loads generated on the airframe and, hence, on the steady performance, flight dynamics, and vibratory characteristics of the aircraft. Houston and Tarttelin[7] used a dynamic inflow-type model to identify some of the stability derivatives from measurements of the heave dynamics of a hovering helicopter. Discrepancies in their analysis were attributed to the unmodeled effects of nonuniform inflow near the rotor resulting from interference from the tail rotor with the locations of the tip vortices of the main rotor blades. Padfield and DuVal[8] have suggested that their problems in identifying stability derivatives in forward flight were also attributable to the effects of unmodeled tail rotor and main rotor interactions. Numerical studies, such as Rosen and Isser's[9] use of a prescribed-wake model to identify the orientation of the rotor blades relative to the vorticity in the wake as a key factor in improving the prediction of the off-axis response of the rotor, support a requirement for improved fidelity of the wake models used in flight dynamics applications.

An important physical limitation on the performance of high-fidelity flight dynamic models is imposed by the disparity in the timescales associated with the rotor dynamics and aerodynamics and the timescale associated with the fuselage motions of the rotorcraft. The blade–wake interactional aerodynamic effects of most relevance to improved modeling fidelity occur on a timescale associated with the rotational frequency of the rotor. The wake structures generated by these interactions then convect away from the interaction sites at roughly the flight speed of the helicopter. Because the body dynamics and wake-convection effects have characteristic frequencies roughly an order of magnitude smaller than the rotor frequencies, an element of stiffness is introduced, resulting in large computational times for any flight dynamic simulation that is detailed enough to resolve the most important blade–wake interactional aerodynamic effects.

A grid-based, Eulerian approach, in particular when the governing fluid dynamic equations are cast into a form that explicitly enforces conservation of vorticity, remains the most natural choice to adopt in the present context. First, coalescence and rupture of domains of vorticity, as are often encountered in strongly interactive flows, are naturally handled by such an approach, implying that wake structures of almost arbitrary complexity should be able to evolve within the computational domain. Additionally, an increase in the size of the cells used to tessellate the computational domain should result merely in a degradation in the resolution of the vorticity in the wake that should ultimately manifest itself merely as a degradation in the resolution of the loading on the rotors and airframe. In the flight dynamics context where often only the integrated loads on the airframe are of direct interest, this structural stability of the wake model should, within reason, imply the relative insensitivity of the numerical values of these loads to the level of resolution of the wake structure.

Received 8 February 1999; revision received 24 June 1999; accepted for publication 3 July 1999.

*Postdoctoral Research Assistant, Department of Aerospace Engineering; currently Lecturer, Department of Aeronautics, Imperial College of Science, Technology and Medicine, Prince Consort Road, London, England SW7 2BY, United Kingdom.

In recent years several impressive grid-based techniques for the numerical solution of the Euler or Navier–Stokes equations for the flow surrounding complete rotor configurations have indeed been developed. The approaches of Strawn and Barth[10] and Raddatz and Pahlke,[11] among others, are typical of detailed calculations of blade pressure and velocity distributions required for accurate calculation of the aerodynamic, structural, and acoustic properties of modern rotor blades. Techniques of this sophistication are not likely to be practical for flight dynamics purposes for some time to come. There are outstanding issues, such as the loss of accuracy[12,13] induced by the tendency of grid-based methods to dissipate any vortical structures present in the flow, that represent particularly severe handicaps in rotorcraft applications given the concentrated structure of the vorticity in the wake. The limitation imposed by the already extreme computational time requirements of techniques based on the direct solution of the Euler or Navier–Stokes equations must also be resolved[14] before these methods are accepted into use in flight dynamic applications.

In this paper, a grid-based, Eulerian formalism, ultimately founded on the solution of the Navier–Stokes equation in vorticity conservation form, is presented for the calculation of the unsteady aerodynamic environment surrounding a helicopter rotor system. The approach addresses, with success, the deficiency inherent in the present generation of Eulerian codes associated with the diffusion of vortical structures into the computational domain. In addition, the vorticity conservation approach adopted here admits a natural decomposition of the evolution of the wake structure, allowing the characteristic stiffness introduced into the rotorcraft flight dynamic problem by disparate rotor and body/wake timescales to be overcome. These favorable characteristics of the vorticity-conservation approach in the context of helicopter flight dynamic modeling are confirmed by application to several model problems. Then, as a prelude to full implementation of the technique in a comprehensive model of the flight dynamics of rotorcraft, the predictions of the resultant rotor wake model are validated against available data for an isolated rotor and for a case where there are strong rotor–wake interactions.

Helicopter Wake

Let V be the volume occupied by the vehicle and its surrounding flowfield. Adopt the classical, asymptotically inviscid, aerodynamic approach that, at any time t, the generation of aerodynamic forces occurs in some subset $B(t)$ of V whereas in the remainder of V the flow behaves in an essentially inviscid manner. The analysis of the flow in V is, thus, decomposed into an outer, wake evolution, problem and an inner problem involving the generation of the aerodynamic forces on the vehicle. Let the loading on, and the subsequent motions of, the airframe and rotors be described by the evolution of some state vector $\boldsymbol{b}(t)$.

Define the vorticity $\omega(\boldsymbol{x}, t)$ at $\boldsymbol{x}$ in V in terms of the velocity $v(\boldsymbol{x}, t)$ of the flow as

$$\omega = \nabla \times v \tag{1}$$

Assuming incompressibility, a Poisson equation

$$\nabla^2 v = -\nabla \times \omega \tag{2}$$

relates the velocity and vorticity of the flow. The evolution of an outer flow governed by the Navier–Stokes equations, reduced by assuming the flow to be inviscid and incompressible, is described in terms of the transport of the vorticity in V by

$$\frac{\partial}{\partial t}\omega + v \cdot \nabla\omega - \omega \cdot \nabla v = S[\boldsymbol{b}(t)] \tag{3}$$

Under the initial assumption that the computation of the flow surrounding the rotorcraft can be decomposed into inner and outer aerodynamic problems, the source term S is nonzero only in $B(t)$ and the dynamics of the airframe and rotor enters the computation only through the dependence of the source term on the state vector $\boldsymbol{b}(t)$. The source term effectively couples the inner and outer problems, and the mismatch in timescales in the flight dynamic problem appears in this formulation purely as a mismatch between the timescale associated with the evolution of ω in the absence of sources and the timescale associated with the evolution of $\boldsymbol{b}(t)$ and, thus, S.

Numerical Implementation

Construct a computational domain V' placed so that it surrounds the aircraft and partially encloses the flow in which the vehicle is immersed. Tessellate V' by a finite number N of three-dimensional cells V_i'. A form of Eq. (3) that explicitly expresses the conservation of vorticity follows in standard fashion by integrating in a piecewise fashion over the cellular structure of V':

$$[\omega]^{n+1} - [\omega]^n = [v \cdot \nabla\omega]^n_{\Delta t} + [S]^n_{\Delta t} - [\omega \cdot \nabla v]^n_{\Delta t} \tag{4}$$

where, for any flow variable $q(\boldsymbol{x}, t)$,

$$[q]^n = \int_{V_i} q(\boldsymbol{x}, n\Delta t)\, \mathrm{d}\boldsymbol{x} \tag{5}$$

$$[q]^n_{\Delta t} = \int_n^{(n+1)\Delta t} [q]_n\, \mathrm{d}t \tag{6}$$

on discretizing time as $t = n\Delta t$ where $n = 0, 1, \ldots$. The total vorticity contained within each computational cell V_i' at timestep n is $[\omega]^n$. The vorticity transported into V_i' and the vorticity produced as a result of stretching by the flow are, respectively, $[v \cdot \nabla\omega]^n_{\Delta t}$ and $[\omega \cdot \nabla v]^n_{\Delta t}$, whereas the total source of vorticity within V_i' between timesteps n and $n+1$ is $[S]^n_{\Delta t}$.

Given the initial vorticity distribution $[\omega]^0$ in the wake, the sequence $[\omega]^n$, $n = 1, 2, \ldots$, generated by the explicit procedure

$$\begin{aligned} v^n &= v([\omega]^n) \\ [\omega]^* &= [\omega]^n + [v \cdot \nabla\omega]^n_{\Delta t}([\omega]^n, v^n) - [\omega \cdot \nabla v]^n_{\Delta t}([\omega]^n, v^n) \\ [\omega]^{n+1} &= [\omega]^* + [S]^n_{\Delta t}(\boldsymbol{b}(n\Delta t), v^n) \end{aligned} \tag{7}$$

yields an order Δt^2 time-accurate approximation[15] to the vorticity obtained from Eq. (4), provided that the various operators comprising this procedure are all themselves at least second-order time-accurate approximations to the operators in Eq. (4). Most importantly, this procedure is stable if each of the operators is allowed to advance within its own particular stability limit.[15]

Equation (7) has been implemented in the code RAGD. The operator $v([\omega]^n)$ yields an approximation to the solution v of Eq. (2), in RAGD, calculated using a Poisson solver based on Schumann and Sweet's[16] method of cyclic reduction. This approach is significantly faster than evaluation of the operator via the Biot–Savart integral, but further increases in the computational speed of this part of the algorithm may be possible using a suitable adaptation of one of the the fast-multipole techniques[17,18] currently reaching maturity. The stretching operator $[\omega \cdot \nabla v]^n_{\Delta t}$ is then approximated by Runge–Kutta integration over a single computational timestep.

The present implementation uses Toro's[19] weighted average flux (WAF) method, extended to three dimensions using the standard Strang spatial splitting,[20] to approximate the transport operator $[v \cdot \nabla\omega]^n_{\Delta t}$. The WAF method is a conservative Riemann problem-based method that can be modified to use flux limiter functions to create solutions that preserve the monotonicity of $[\omega]^n$ at each timestep. Although the technique was developed to enable the accurate resolution of discontinuities in compressible flows, here the use of flux limiter functions in a conservative formulation allows the compactness of the domains of vorticity in the flowfield to be controlled while still conserving the total vorticity present in the computational domain.

The mismatch of timescales inherent in the flight dynamic problem results in the timestep required to maintain the accuracy and stability of $\boldsymbol{b}(t)$ generally being very much smaller than the timestep Δt at which Eq. (7) can be advanced in the absence of vorticity sources. The impact of this stiffness on the execution time of the algorithm can be reduced by modifying the structure of the source term to effectively decouple the rate of advance of the inner and outer problems as follows. The conservative structure of Eq. (7)

allows the vorticity source to be approximated as $[S]^n_{\Delta t} = [S]^{n^*}_M$ on defining a sequence of intermediate sources of vorticity:

$$[S]^{n^*}_m = [S]^{n^*}_{m-1} + [S]^{n+m/M}_{\Delta t/M}(\boldsymbol{b}(n\Delta t + m\Delta t/M), v^n + v^*_m) \quad (8)$$

if $0 < m \leq M$, on defining $[S]^{n^*}_0 = 0$, and where v^*_m is a correction to the velocity field to account for the source of vorticity during intermediate steps $1, \ldots, m-1$. The inner calculation is now effectively advanced at timestep $\Delta t/M$, and the number of substeps M can be selected to be large enough to maintain the accuracy of the vorticity source and the stability of the algorithm used to calculate $\boldsymbol{b}(t)$. Note, though, that M must still be kept small enough to avoid the averaging process inherent in the construction of the total vorticity source from the intermediate sequence from obliterating spatial features in the wake that are of relevance to the problem at hand. The computational time saving resulting from suitable factorization of the source term can be readily estimated. If t_i and t_o are the times spent, per timestep, respectively, on performing the inner and the outer calculations, then the total computational time spent per timestep if the inner problem is factored into M steps is $Mt_i + t_o$ because the solution to the outer problem need only be advanced once for every M times the solution to the inner problem is advanced, compared to $M(t_i + t_o)$ for a computation without factorization where the rate of advance is limited by the inner calculation. Factorization of the source term, thus, yields a time saving of $(M-1)t_o$ per timestep. The sensitivity of the computed solution to the number of substeps used to advance the solution to the inner problem is illustrated later.

Although a similar approach to the construction of the source operator would follow the adoption of a more comprehensive theory of loads generation (for instance one incorporating fully three-dimensional, viscous, or compressible aerodynamic effects), for illustration, the inner model is constructed here by assuming the aerodynamic forces on the vehicle to result from a distribution of bound vorticity ω_b confined to the neighborhood of the blades. Continuity of vortex lines requires the bound vorticity to be accompanied by a source of vorticity:

$$S_b = -\frac{\mathrm{d}}{\mathrm{d}t}\omega_b + v_b \nabla \cdot \omega_b \quad (9)$$

into the surrounding fluid, where v_b is the velocity of the bound vorticity relative to the fluid. The two terms of this source are, respectively, the shed and trailed vorticity from the blades. As a further simplification, assume the bound vorticity is concentrated on the quarter-chord lines of the blades. The deficiencies of this lifting-line approximation are discussed by van Holten,[21] but the approach is still widely used in the helicopter community. Each blade is divided into a number of spanwise elements, each with its own collocation point at which the local velocity interpolated from the computational grid, the velocity v^*_m associated with the vorticity shed and trailed from the blade during the current timestep, and the section angle of attack are combined to yield the local loading on the blade. The spanwise variation of loading and the rate of change of spanwise loading with time result in a source of vorticity into the computational domain given by Eq. (9). The source of vorticity from each blade is then mapped onto an interpolating surface representing the (convected) trajectory of the blade during the current timestep. Finally, the vorticity source $[S]^{n^*}_m$ is obtained by transferring the vorticity from the interpolating surface into the computational domain by integration over the intersection between the interpolation surface and each of the computational cells.

Results

The results of a series of computations performed to validate the algorithm and to illustrate the potential of RAGD are now presented. In all cases a cubic computational domain, tessellated into equal-sized cubic cells, was used to capture the vorticity in the rotor wake. Potential improvements in the performance of the code that might result from local grid refinement or distortion of the cells to match better the inherent geometry of the rotors and wake will not be investigated in this paper. Throughout, zero-curvature conditions were simultaneously imposed on the vorticity and velocity on all boundaries of the computational domain. The ill-posed nature of Eq. (2) with these boundary conditions is resolved by collocation with the velocity evaluated by the conventional Biot–Savart integral at a single, quiescent, point in the flow. This approach would appear to yield the best compromise between allowing vorticity to convect through the boundaries with minimal propagation of disturbances back into the computational domain and proper representation of far-wake effects on the velocity field.

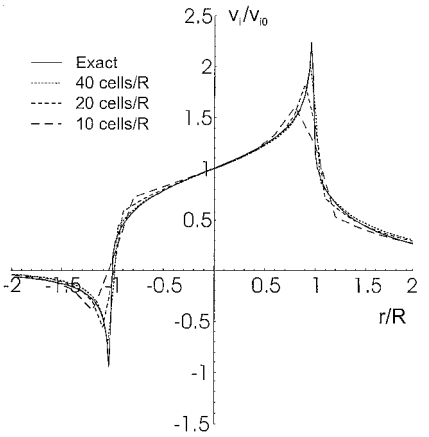

Fig. 1 Structural stability of induced velocity.

Structural Stability

The structural stability of the solutions generated by RAGD to changes in the resolution of the vorticity in the wake is illustrated by computing the induced velocity for the Coleman et al. simplified model of an isolated rotor in forward flight.[22] Assume that the rotor has an infinite number of uniformly loaded blades, and assume that the rotor is moving through the surrounding fluid at high speed relative to the induced velocity generated by the rotor and its wake. The wake structure then consists of a cylindrical sheet, together with an axial vortex filament, both inclined to be parallel to the direction of motion of the rotor through the surrounding fluid, on which the vorticity has constant magnitude. The simple wake structure allows the wake-induced velocity in the neighborhood of the rotor to be obtained analytically and to be compared with results obtained using the numerical algorithm with the rotor radius resolved over 40, 20, and 10 computational cells. Figure 1 shows the induced velocity component v_i perpendicular to the rotor disk, normalized by the induced velocity v_{i0} at the center of the rotor disk, on the longitudinal plane of a rotor that is climbing at an angle of 45 deg to its axis through the surrounding fluid. Reduction in the number of cells used to resolve the rotor results in a loss of resolution of the wake structure for the same source of vorticity into the flow. Importantly, though, reduction in the resolution of the vorticity in the computational domain results merely in a reduction in the resolution of the induced velocity on the rotor disk and not in a change in the solution to a form that is qualitatively different from that obtained with a more finely resolved wake structure. Features in the induced velocity on a scale comparable to the size of the computational cells are simply not resolved. In addition to illustrating the structural stability of the procedure to changes in grid resolution, this example also serves to confirm the important property of convergence of the algorithm on the exact solution to the problem as the size of the computational cells is reduced.

Time Factorization

The behavior of the time-factorization algorithm is illustrated by configuring RAGD to calculate a numerical approximation to the analytic solution for Theodorsen's (see Ref. 23) linearized model of a blade element oscillating sinusoidally in pitch about its half-chord. Define the reduced frequency of the pitching oscillation $k = vc/(2U)$, then in general $C_L = C(k)C^*_L$, where C^*_L is the lift coefficient for the airfoil in the quasistatic limit $v/U \rightarrow 0$, C_L is the lift coefficient for the airfoil under dynamic conditions, and C is known as the lift deficiency function. The RAGD code is easily modified to satisfy the assumptions of Theodorsen's analysis by allowing the shed wake to convect under the influence of the

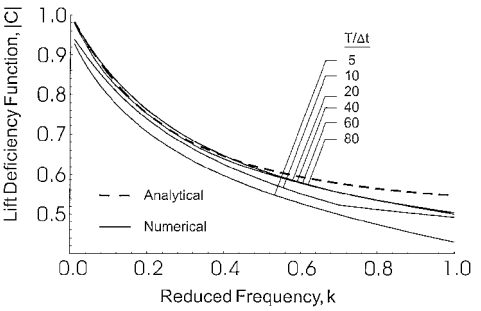

a) Analytical and numerical solutions with no factorization

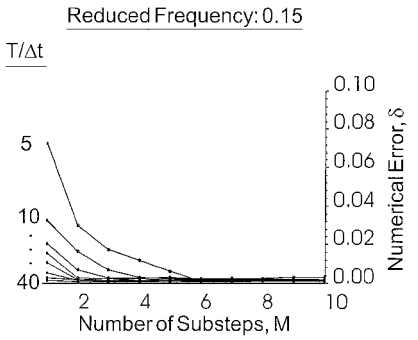

b) Effect of source factorization on numerical error

Fig. 2 Airfoil oscillating in pitch.

freestream alone (hence neglecting any self-induced wake distortion) and by appropriate reduction of the governing equations and discretization from three dimensions to two. Figure 2a shows the variation of the amplitude of Theodorsen's lift deficiency function with reduced frequency, calculated using the RAGD code with no factorization of the source term ($M = 1$) and for various ratios of computational timestep Δt to oscillation period $T = 2\pi/\nu$. Convergence to a fixed solution for small values of $\Delta t/T$ is seen, but the numerical solution diverges significantly from the exact result for larger reduced frequencies. This behavior is shown by Miller[24,25] to be consistent with the use of lifting-line theory in place of Theodorsen's lifting-surface inner aerodynamic model. Figure 2b shows the effect on the numerical solution of time factorization of the source term. The error between the solution computed with a varying number M of substeps and the converged numerical solution, normalized by the converged numerical value for the lift deficiency function, is shown for various $\Delta t/T$. Although Fig. 2 is drawn for $k = 0.15$, the observed behavior is typical of all $0 < k < 1$. The results presented here for this simple model problem show that the accuracy of a calculation performed at a timestep too large to resolve the dynamics of the inner flow can be restored by selection of a suitable number of substeps for calculation of the inner model and, hence, that factorization of the vorticity source can indeed be used to alleviate the stiffness introduced by the disparate rotor and wake timescales.

Vorticity Confinement

To illustrate the effects of various strategies for overcoming the adverse effects of numerical diffusion on the resolution of the vorticity in the wake, the RAGD code is used to calculate the wake structure for a rotor of solidity 0.1, consisting of three blades with constant chord and a linear twist of 12 deg, advancing axially at 0.35 times the blade tip speed at a thrust coefficient of 0.088. The wake structure for this simple case should consist of a set of helical vortices trailing from the tips of the rotor blades and propagating downstream of the rotor without significant change in strength, together with a much weaker system of vortices trailing downstream inboard of the tip system. The rotor was placed at the center of a cubic computational domain that resolved the rotor radius across 10 cells, and the WAF algorithm with flux limiter functions defined by Toro[26] was used to construct the transport operator of the split algorithm. Figure 3 shows the instantaneous position, for two different cases, of one of the surfaces on which the vorticity in the wake of

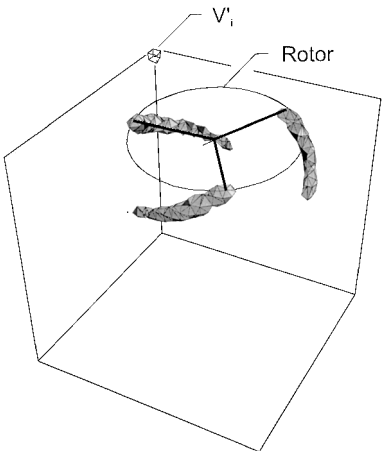

a) MIN-type flux limiter: computational cell V_i' is the smallest resolveable feature in the flow

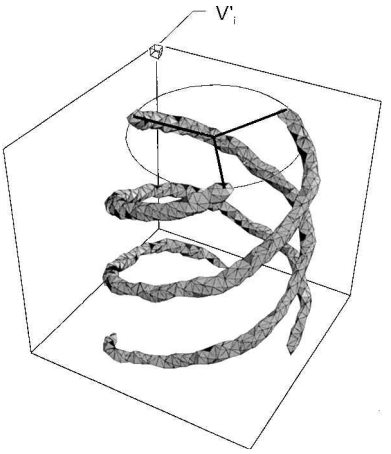

b) SUPER-type flux limiter

Fig. 3 Effect of flux-limiting routine on wake structure.

the rotor has constant magnitude. The magnitude of the vorticity on the plotted surface is sufficiently large that only the helical tip vortices should be strong enough to appear.

The WAF algorithm in conjunction with a MIN-type limiter is only mildly confining in its action on the wake vorticity, as is illustrated in Fig. 3a by the rapid dissipation of the tip vortices a short distance downstream of the rotor. The observed behavior is characteristic of monotonicity-preserving, grid-based solvers that allow only very small excursions from the second-order time accuracy of the basic WAF method. Figure 3b shows the improvement in confinement that can be obtained by suitable modification to this basic approach. The same system is modeled using the WAF routine, but this time with the MIN-type limiter replaced by an extremely compressive SUPER-type limiter. The success of the present approach at maintaining the strength of the tip vortices all of the way to the edge of the computational domain and, indeed, in confining the vorticity down to the minimum scale resolveable by the computational grid, is evident.

Illustrative Cases

A number of examples that serve to validate the accuracy of the approach adopted in the RAGD code are now presented. In all cases the calculation was advanced at a timestep for the outer computation of $\frac{1}{60}$th of the rotor period, while the inner calculation was factorized into 10 substeps. On a cubic grid resolving the rotor radius across 10 cells, this level of resolution resulted in computational times ranging between 600 and 1500 s per rotor revolution on a Pentium 166-MHz machine with 32 MB of RAM, compared to between 5000 and 6000 s per rotor revolution for a calculation with no factorization of the inner calculation. Throughout the following calculations, a SUPER-type limiter was used in the convective component of the algorithm.

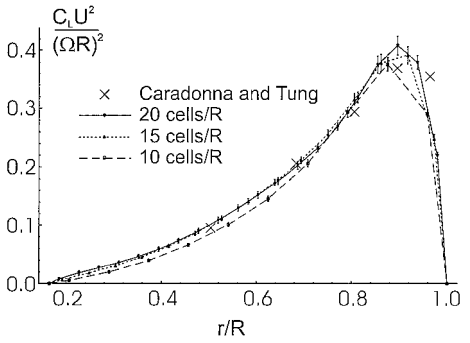

Fig. 4 Isolated rotor in hover, blade load distribution.[28]

Wake Structure in Hover

In this section, predictions by RAGD of blade spanwise loading and tip-vortex geometry are compared against the widely used[10,27] benchmark provided by Caradonna and Tung's[28] experimental data for a rotor consisting of two blades with aspect ratio 6 and zero twist, in hover at a collective pitch setting of 12 deg. Figure 4 shows structurally stable convergence of the loading on the blades as the resolution of the computational grid and number of aerodynamic collocation points along the blade is increased. In each case the number of collocation points along the blade was set equal to the number of cells used to resolve the rotor radius, and the collocation points were spaced equally along the length of the blade. No attempt was thus made to optimize the representation of the blade loading, for instance by clustering collocation points in regions of high, spanwise loading gradients. A slight unsteadiness in the calculated loading is indicated by plotting the mean loading over 14 rotor revolutions, with the error bars denoting a single standard deviation of the loading from the mean.

The converged numerical loading distribution shows satisfactory correlation with Caradonna and Tung's experimental data,[28] although the predicted position of maximum loading is slightly inboard of the experimentally suggested position. Figure 5 shows contour plots of the magnitude of the wake vorticity component normal to a plane containing the rotor axis, calculated on computational grids resolving the rotor radius over 10, 15, and 20 cells. The pattern shown is typical of the instantaneous distribution of the vorticity in the wake; the positions of the centers of the tip vortices can be identified as local maxima in the vorticity plots. Although the calculation at the lowest resolution is too coarse to resolve individual tip vortices, good agreement between the calculated vortex core positions close to the plane of the rotor and the experimental correlations of tip vortex geometry constructed by Kocurek and Tangler[29] is obtained once the spatial resolution of the wake structure becomes sufficient to resolve the positions of individual vortex cores. Note, though, that the numerical results show the concentrated and relatively stable vortex structure close to the rotor to break down after approximately two rotations of the rotor and to be replaced with a less-concentrated structure that is asymmetrically placed with respect to the axis of the rotor. Further analysis shows the asymmetry of this far wake to vary erratically with time. The general features of the instability appear to be relatively insensitive to cell size (as well as to the overall size of the computational domain) and to the position of the rotor within the computational domain, strongly suggesting that the observed structure is inherent in the fluid dynamics rather than being merely an artifact of the computational scheme. Interestingly, the present approach would appear to model, at least qualitatively, some of the unsteady dynamics and instability of the hovering rotor's far wake reported by Leishman and Bagai,[30] although further investigation of the finer details of the causes and development of the observed instability is warranted.

Wake Interaction

Akimov et al.[31] have attempted to resolve the interacting wake structure generated by twin, coaxial, contrarotating rotors by injecting smoke into the flow near the tips of the rotor blades of an in-flight Kamov Ka-32 helicopter at a variety of advance ratios. Bagai and Leishman[32] have compared the predictions of their free-wake code

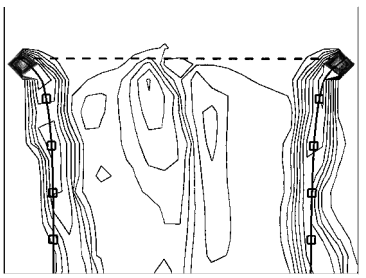

10 cells/*R*

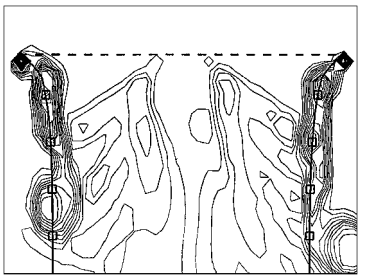

15 cells/*R*

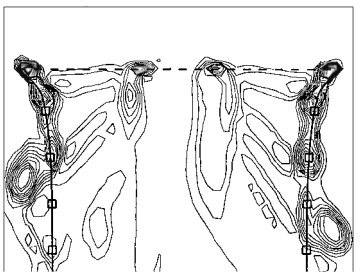

20 cells/*R*

Fig. 5 Isolated rotor in hover, vorticity distribution in wake: - - - -, rotor TPP; Kocurek and Tangler[29] correlation: ——, wake envelope; and □, tip vortex position.

to the experimental data and, in addition, have clearly identified several interactional effects in the tip vortex geometries generated by their technique. These analyses can be used together to verify simultaneously the wake structure generated by the present approach in forward flight as well as in a case where strong interactions are to be expected. To create a computational analog of the experimental approach adopted by Akimov et al., the trajectories of a series of particles released from the tips of the blades were tracked as they were transported along with the flow through the computational domain. It should, of course, be borne in mind that the trajectories of smoke or computational particles do not necessarily represent faithfully the structure of the vorticity in the wake, complicating somewhat the comparison between the results of the three separate approaches. Figure 6a shows particle trajectories for the upper and lower rotors calculated for zero advance ratio, whereas Fig. 6b shows comparisions of the calculated and experimentally determined wake profile along a longitudinal axis through the helicopter fuselage, also for the system in hover. Figure 7 shows similar information for the system at an advance ratio of 0.089.

In hover, the increased axial distortion and subsequent contraction of the wake of the upper rotor, and converse behavior of the wake of the lower rotor, are similar to that observed in the previous studies. The present approach suggests, however, that merging of the individual rotor wakes does indeed eventually take place but that it is associated with the onset of wake instability at about 1.5 rotor diameters below the rotors. This instability occurs well outside the limits of observation of both previous studies.

Both the free-wake calculations and the current method show that, in forward flight, the wake from the upper rotor is drawn down toward the wake of the lower rotor. The sides of the two wake cylinders then roll up to form a single pair of trailing vortices extending downstream of the helicopter. Good agreement between the two

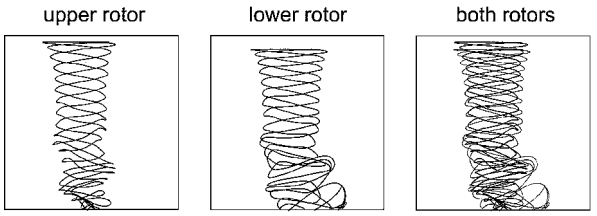

a) Simulated tip-vortex trajectories

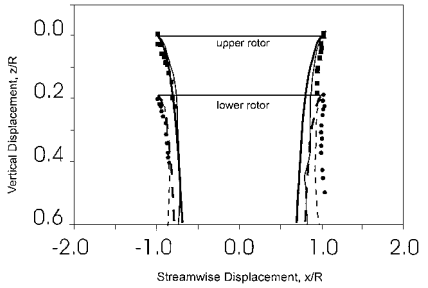

b) Wake sectioned along helicopter centerline

Fig. 6 Interacting rotors in hover. Upper rotor wake: ——, Bagai and Leishman[32]; ——, present approach; and ■, Akimov et al.[31] Lower rotor wake: - - - -, Bagai and Leishman; – – –, present approach; and ●, Akimov et al.

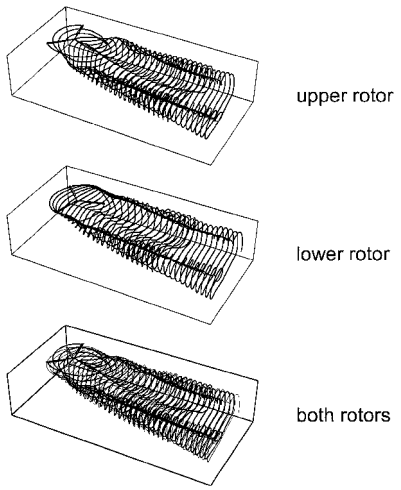

Simulated tip-vortex trajectories

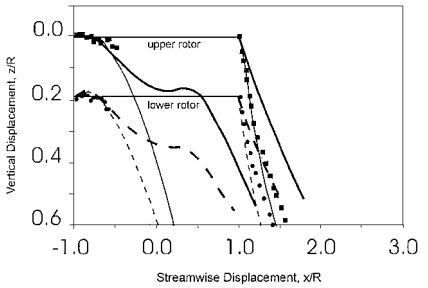

Wake sectioned along helicopter centerline

Fig. 7 Interacting rotors at advance ratio 0.089. Upper rotor wake: ——, Bagai and Leishman[32]; ——, present approach; and ■, Akimov et al.[31] Lower rotor wake: - - - -, Bagai and Leishman; – – –, present approach; and ●, Akimov et al.

approaches extends to the prediction of the blade–wake interaction on the forward sector of the lower rotor, where the wake is initially convected above the plane of the rotor. The principal difference between the wake structures generated using the free-wake approach and the present method is the prediction by the current approach of a distinctive double-trough-type structure in the wake originating from the forward halves of the advancing rotor disks. The free-wake calculations suggest much less severe distortion of this part of the wake, and the discrepancy manifests itself as a significant divergence between the two predicted profiles for the forward boundary of the wake. The double-trough structure most likely has its origin in the induced velocity distribution peculiar to the blades with very large root cutout used on the Ka-32 helicopter. Unfortunately, the structure of this part of the wake generated by the isolated rotors cannot be resolved from the experimental data because of interference from the rotor mast and fuselage.

Conclusions

A computational rotor wake model based on the numerical solution of the unsteady fluid-dynamic equations governing the generation and convection of vorticity through a domain enclosing the rotorcraft has been developed. The model addresses issues of specific interest to the modeling of the dynamic behavior of rotorcraft. Using a vorticity-conservation approach, the tendency of conventional, domain-based approaches to disperse regions of concentrated vorticity is successfully addressed by using flux limiting functions to control the convection of vorticity through the domain. In addition, the characteristic disparity between the timescales associated with the rotor dynamics and aerodynamics and the timescales associated with the fuselage motions and wake convection is dealt with by factorizing the calculation of the blade aerodynamics, and hence the vorticity source into the computational domain, into a sequence of intermediate steps. The wake model presented has been demonstrated to possess favorable properties when applied to a number of model problems and, in addition, valid wake structures in a hover and forward flight for both isolated and interacting rotors have been presented. It is claimed that the intrinsic ability of the approach to deal with situations in which there are strong interactional effects suggests that the approach adopted here may well yield a suitable rotor wake model for the next generation of helicopter flight dynamic models. Ongoing research involves the incorporation of the wake model presented into a comprehensive model for the dynamics of the complete rotorcraft system[5] that includes the motion of the fuselage and blades of multiple rotors.

Acknowledgments

The research leading to this paper was conducted under the ongoing U.K. Engineering and Physical Sciences Research Council Grant GR/L 19614. The author would like to thank Stewart Houston and Frank Coton for motivating the project and for their valuable input during the development of the RAGD code.

References

[1]Carpenter, P. J., and Fridovich, B., "Effect of a Rapid Blade-Pitch Increase on the Thrust and Induced-Velocity Response of a Full-Scale Helicopter Rotor," NACA TN 3044, 1953.

[2]Gaonkar, G. H., and Peters, D. A., "A Review of Dynamic Inflow Modeling for Rotorcraft Flight Dynamics," *Vertica*, Vol. 12, No. 3, 1988, pp. 213–242.

[3]Peters, D. A., Boyd, D. D., and He, C. J., "Finite-State Induced-Flow Model for Rotors in Hover and Forward Flight," *Journal of the American Helicopter Society*, Vol. 34, No. 4, 1989, pp. 5–17.

[4]Chen, R. T. N., "A Survey of Nonuniform Inflow Models for Rotorcraft Flight Dynamics and Control Applications," *Vertica*, Vol. 14, No. 2, 1990, pp. 147–184.

[5]Houston, S. S., "Rotorcraft Aeromechanics Simulation for Control Analysis: Mathematical Model Definition," Dept. of Aerospace Engineering, Rept. 9123, Univ. of Glasgow, Glasgow, Scotland, U.K., 1991.

[6]Turnour, S. R., and Celi, R., "Modelling of Flexible Rotor Blades for Helicopter Flight Dynamics Applications," *Journal of the American Helicopter Society*, Vol. 41, No. 1, 1996, pp. 52–61.

[7]Houston, S. S., and Tarttelin, P. C., "Validation of Mathematical Simulations of Helicopter Vertical Response Characteristics in Hover," *Journal of the American Helicopter Society*, Vol. 36, No. 1, 1991, pp. 45–57.

[8]Padfield, G. D., and DuVal, R. W., "Application Areas for Rotorcraft System Identification Simulation Model Validation," LS138, AGARD, 1991, pp. 12.1–12.39.

[9]Rosen, A., and Isser, A., "A Model of the Unsteady Aerodynamics of a Hovering Helicopter Rotor that Includes Variations of the Wake Geometry," *Journal of the American Helicopter Society*, Vol. 40, No. 3, 1995, pp. 6–16.

[10]Strawn, R. C., and Barth, T. J., "A Finite-Volume Euler Solver for Computing Rotary-Wing Aerodynamics on Unstructured Meshes," *Proceedings of the American Helicopter Society 48th Annual Forum*, American Helicopter Society, Alexandria, VA, 1992, pp. 419–429.

[11]Raddatz, J., and Pahlke, K., "3D Euler Calculations of Multibladed Rotors in Hover: Investigation of the Wake Capturing Properties," CP-552, AGARD, 1995, pp. 13.1–13.16.

[12]Johnson, W., "Recent Developments in Rotary-Wing Aerodynamic Theory," *AIAA Journal*, Vol. 24, No. 8, 1986, pp. 1219–1244.

[13]Landgrebe, A. J., "New Directions in Rotorcraft Computational Aerodynamics Research in the U.S.," CP-552, AGARD, 1995, pp. 1.1–1.12.

[14]Wake, B. E., and Baeder, J. D., "Evaluation of a Navier–Stokes Analysis Method for Hover Performance Prediction," *Journal of the American Helicopter Society*, Vol. 41, No. 1, 1996, pp. 7–17.

[15]Brown, R. E., "Numerical Solution of the Two-Dimensional Navier–Stokes Equations Using Viscous-Convective Operator Splitting," M.Sc. Thesis, College of Aeronautics, Cranfield Inst. of Technology, Cranfield, England, U.K., 1990.

[16]Schumann, U., and Sweet, R. A., "A Direct Method for the Solution of Poisson's Equation with Neumann Boundary Conditions on a Staggered Grid of Arbitrary Size," *Journal of Computational Physics*, Vol. 20, No. 2, 1976, pp. 171–182.

[17]Winckelmans, G. S., and Leonard, A., "Contributions to Vortex Particle Methods for the Computation of 3-Dimensional Incompressible Unsteady Flows," *Journal of Computational Physics*, Vol. 109, No. 2, 1993, pp. 247–273.

[18]Salmon, J. K., Warren, M. S., and Winckelmans, G. S., "Fast Parallel Tree Codes For Gravitational and Fluid Dynamical N-Body Problems," *International Journal of Supercomputer Applications and High Performance Computing*, Vol. 8, No. 1, 1994, pp. 129–142.

[19]Toro, E. F., "A Weighted Average Flux Method for Hyperbolic Conservation Laws," *Proceedings of the Royal Society of London, Series A: Mathematical and Physical Sciences*, Vol. 423, No. 1864, 1989, pp. 401–418.

[20]Billett, S. J., and Toro, E. F., "On WAF-Type Schemes for Multidimensional Hyperbolic Conservation Laws," *Journal of Computational Physics*, Vol. 130, No. 1, 1997, pp. 1–24.

[21]van Holten, T., "On the Validity of Lifting Line Concepts in Rotor Analysis," *Vertica*, Vol. 1, No. 3, 1977, pp. 239–254.

[22]Coleman, R. P., Feingold, A. M., and Stempin, C. W., "Evaluation of the Induced Velocity Field of an Idealized Helicopter Rotor," NACA ARR-L5E10, 1945.

[23]Johnson, W., *Helicopter Theory*, Princeton Univ. Press, Princeton, NJ, 1980.

[24]Miller, R. H., "Unsteady Air Loads on Helicopter Rotor Blades," *Journal of the Royal Aeronautical Society*, Vol. 68, No. 640, 1964, pp. 217–229.

[25]Miller, R. H., "Rotor Blade Harmonic Air Loading," *AIAA Journal*, Vol. 2, No. 7, 1964, pp. 1254–1269.

[26]Toro, E. F., *Riemann Solvers and Numerical Methods for Fluid Dynamics: A Practical Introduction*, 2nd ed., Springer–Verlag, New York, 1999.

[27]Brown, K. D., and Fiddes, S. P., "New Developments in Rotor Wake Methodology," *Proceedings of the Twenty-Second European Rotorcraft Forum*, Royal Aeronautical Society, London, 1996, pp. 14.1–14.12.

[28]Caradonna, F. X., and Tung, C., "Experimental and Analytical Studies of a Model Helicopter Rotor in Hover," *Vertica*, Vol. 5, No. 2, 1981, pp. 149–161.

[29]Kocurek, J. D., and Tangler, J. L., "A Prescribed Wake Lifting Surface Hover Performance Analysis," *Journal of the American Helicopter Society*, Vol. 22, No. 1, 1977, pp. 24–35.

[30]Leishman, J. G., and Bagai, A., "Challenges in Understanding the Vortex Dynamics of Helicopter Rotor Wakes," *AIAA Journal*, Vol. 36, No. 7, 1998, pp. 1130–1140.

[31]Akimov, A. I., Butov, V. P., Bourtsev, B. N., and Selemenev, S. V., "Flight Investigation of Coaxial Rotor Tip Vortex Structure," *Proceedings of the American Helicopter Society 50th Annual Forum*, American Helicopter Society, Alexandria, VA, 1994, pp. 1431–1449.

[32]Bagai, A., and Leishman, J. G., "Free-Wake Analysis of Tandem, Tilt-Rotor and Coaxial Rotor Configurations," *Journal of the American Helicopter Society*, Vol. 41, No. 3, 1996, pp. 196–207.

K. Kailasanath
Associate Editor